Magnetic behavior of $Mg(Fe,Al)_2O_4$: A Mossbauer study

S. C. Bhargava
Solid State Physics Division, Bhabha Atomic Research Centre, Bombay 400 094, India
(Received 1 December 1997)

Mossbauer study of the mixed ferrites $MgFe_xAl_{2-x}O_4$ ($x=0.75$, 0.9), in the concentration range in which spin-glass ordering is predicted, has been made. A magnetic transition at temperature (25–40 K) much lower than T_N, and anomalous behavior of the ionic magnetization related to this transition, is concluded to be due to fluctuations between energy equivalent noncollinear spin configurations. The nature of spin ordering in the oxide is comparable to the spin-glass ordering. Observable characteristics of spin-glass behavior are deduced. [S0163-1829(98)01330-7]

I. INTRODUCTION

The magnetic behavior of mixed ferrites with a high concentration of diamagnetic ions shows a large number of characteristics which are not yet well understood. The presence of diamagnetic ions on a sublattice has been found to result in noncollinearity of spins on the adjacent sublattice, which increases with the concentration of the diamagnetic ions.[1–5] Due to the short-range nature of the magnetic interactions in oxides, the noncollinearity depends on the number of diamagnetic ions in the immediate neighborhood.[3–5] At larger concentration of the diamagnetic ions, the noncollinearity angle can be greater than 90°, which has been experimentally verified.[6] In such a case, the noncollinear spin ordering of the sublattice is closer to the spin-glass ordering. It has been of great interest to compare the magnetic behavior of such mixed oxides with the high concentration of the diamagnetic ions and canonical metallic spin glasses, to examine the effects of the difference in the nature of magnetic interactions in oxides and metallic systems on the spin-glass behavior.

At higher concentration of the diamagnetic ions, Mossbauer spectroscopy revealed an anomalous behavior of the temperature dependence of ionic magnetization.[7–10] Subsequently, such an anomalous behavior of ionic magnetization was found in canonical metallic spin glass AuFe,[11–14] other oxides,[15,16] and amorphous $Fe_xNi_{78-x}Si_9B_{13}$ also.[17] The behavior observed in the metallic systems and oxides, however, differ significantly. In the case of the metallic systems, the shape of the anomalous temperature dependence does not change on application of an external magnetic field. In oxides, on the other hand, the anomaly in the temperature dependence of $\langle S_Z \rangle$ decreases when an external field is applied. Even a small external field has been found to reduce the anomalous behavior[7–10] appreciably. It is not clear if this difference in the effect of the magnetic field is due to the difference in the magnetic nature of oxides and metallic systems or if the origin of the anomaly in the two cases is different.

Finally, at high concentration of the diamagnetic ions, superparamagnetic effects are necessarily present in insulator oxides due to the short-range nature of the magnetic interactions.[18]

These properties of the mixed oxides have been extensively investigated using Mossbauer spectroscopy as well as ac and dc magnetization measurements. The temperature dependence of the ac susceptibility of the mixed oxide shows a cusp which is sharper when the concentration of the diamagnetic ions is large. Field-cooled (FC) and zero-field-cooled (ZFC) magnetizations show branching. The branching temperature decreases as the external field increases.[19–21] The hysteresis loop of a mixed ferrite with a significant concentration of diamagnetic ions reveals a rapid increase in the coercive field with the decrease in temperature, at temperatures lower than 30 K. However, these characteristics can be due to superparamagnetism or spin-glass ordering.[22] The presence of superparamagnetic clusters in mixed oxides, even when the particle size is large, makes it difficult to detect the spin-glass characteristics of oxides unambiguously using these macroscopic methods. This is not the case in metallic substances, which do not show superparamagnetic effects when the particle size is large. Superparamagnetism, therefore, does not prevent the observation of spin-glass characteristics in metallic substances using these macroscopic methods.

Mossbauer spectroscopy, on the other hand, can distinguish spin-glass and superparamagnetic effects in oxides, and is, therefore, useful in the study of spin-glass phenomena in oxides. Earlier studies using this method have already revealed several other phenomena in mixed oxides. They showed the presence of ionic spin-relaxation effects, the anomalous temperature dependence of $\langle S_Z \rangle$, and the noncollinearity of spins which has been found to decrease rapidly with the increase in temperature and vanish below the liquid-nitrogen temperature, even if the magnetic transition temperature is much higher.[7–10,15,16] The shapes of the Mossbauer spectra are, however, quite complex due to the presence of dynamical effects. Single-ion spin-relaxation effects are found in the spectra of all mixed ferrites, even at low temperatures. At higher temperatures, below magnetic ordering temperature, superparamagnetic fluctuations appear which lead to the collapse of magnetic splitting below the magnetic transition temperature. At higher temperatures, spin-lattice relaxation also becomes important, which is independent of magnetic ordering of any kind.[23,24] It is, therefore, necessary to analyze the Mossbauer spectra taking into consideration these fluctuation effects.

In the present study, mixed ferrites with a high concentrations of diamagnetic ions, which are expected to show spin-

TABLE I. Results of the analysis of Mossbauer spectrum of $MgFe_{0.9}Al_{1.1}O_4$ at the ambient temperature.

Component 1 (*B* site)				Component 2 (*A* site)			
QS (mm/s)	CS[a]	Γ (mm/s)	RI (%)	QS (mm/s)	CS[a]	Γ (mm/s)	RI (%)
0.81	0.26	0.39	41	0.45	0.24	0.39	59

[a]Center shift relative to Fe metal in mm/s.

glass ordering[22] as well as other complicated magnetic phenomena mentioned above, are studied using Mossbauer spectroscopy. It was predicted[22] that $MgFe_xAl_{2-x}O_4$ with $x < 1.0$ would be a spin glass. In the present study, the oxides with $x = 0.9$ and 0.75 have been investigated using Mossbauer spectroscopy. The measurements are made in zero external field when features characterizing spin-glass behavior are not smeared. The composition has only one type of magnetic ion (Fe^{3+}) only, which has negligible single-ion anisotropy. The spin-glass properties are, therefore, exclusively due to the dilutions of the magnetic ions on the two sites. The spectra are analyzed accurately by taking into consideration the presence of relaxation effects. The effects of various phenomena mentioned above are thus determined. An earlier study of these two oxides[21] showed that the temperature dependences of ZFC and FC magnetizations do not overlap below a temperature. In the case of $x = 0.9$, this branching temperature was found to lower significantly with an increase in the applied field. Such behavior was shown to be due to superparamagnetism.[21] The remnant magnetization and coercivity showed a large increase at temperatures lower than 25 K. Above this temperature the coercivity is 10 Oe. These features were attributed to the spin-glass ordering of the single domain magnetic clusters present in these materials. The dc magnetization does not attain saturation up to the magnetic-field strength of 1.5 T even at 75 K, where the coercivity is quite small.[21] This shows the presence of noncollinearity of moments in this oxide with $x = 0.9$. In the other composition, noncollinearity is expected to be more prominent, due to a larger concentration of diamagnetic ions.

II. EXPERIMENTAL

The oxides were prepared using the conventional ceramic procedure. The desired ratios of the component oxides were thoroughly mixed under alcohol and calcined at 900 °C. The final sintering was done at 1200 °C for 20 h. X-ray analyses showed the presence of single-phase spinel structure in both compositions.

Mossbauer spectra are obtained using a cryogenic setup described elsewhere.[25] Co^{57} in Rh is used as the Mossbauer source. A sine wave is used to drive the spectrometer. The linearization of the spectral velocity scale is done after analyses, for the purpose of presentation only. Both ends of the long drive rod are used to record spectra. One end of the rod carries the source for obtaining calibration spectra using an Fe foil, kept outside the cryostat. The other end of the source carries a stronger source for obtaining the spectra of the oxide under study, inside the cryostat. The two spectra are obtained simultaneously using PC. The widths of the inner lines in the calibration spectrum are ≈0.23 mm/s. The temperature is measured using calibrated carbon glass sensor, and controlled to ±0.1° using an oxford temperature controller (ITC 4).

III. ANALYSES OF EXPERIMENTAL SPECTRA AND RESULTS

Mossbauer paramagnetic spectra at the ambient temperature are fitted with two symmetric doublets. The center shifts (CS) and the quadrupole splittings (QS) of the two doublets are given in Table I. Fe is, thus, found to be in a high-spin Fe^{3+} state at both sites in the two oxides. Using an earlier result[26] that $CS(A) < CS(B)$, and $QS(A) < QS(B)$, the components corresponding to the two sites can be identified. Thus, Fe is found to prefer *A* sites in both cases.

At lower temperatures, magnetic splitting is observed. At 4.2 K, two magnetic component spectra are visible. At higher temperatures, the two magnetic components show the presence of relaxation effects. In addition, a paramagnetic component appears at higher temperatures, which grows in intensity with temperature (Figs. 1 and 2). We, therefore, fit the experimental spectra with a sum of two magnetic component spectra, including the presence of dynamical effects, and a paramagnetic doublet, using the least-squares fit procedure. The magnetic spectrum is calculated using the stochastic model of ionic spin relaxation.[27,28]

A. Ionic spin relaxation

The line shape due to single-ion spin relaxation is given by a simple relation when the ionic Zeeman splitting is large in comparison to the hyperfine splitting, as is the case in magnetic materials. In this case, each of the six nuclear transitions contributes independently to the Mossbauer line shape. The spectral shape of each of the six nuclear transition can be calculated separately and then added with proper weight factors. The spectral shape corresponding to a given nuclear transition is given by[28]

$$I(w) = (2/\Gamma)\mathrm{Re} \sum_{\alpha=1}^{6} iq_\alpha/(w - p_\alpha). \tag{1}$$

Here, the summation is over the six ionic states of the Fe^{3+} ion. Γ is the linewidth in the absence of relaxation effects. p_α are the eigenvalues of the (6×6) matrix **P** with elements

$$P_{\mu\mu'} = (w^\mu - 1/2\, i\Gamma)\,\delta_{\mu\mu'} + iW_{\mu\mu'}. \tag{2}$$

where, $\hbar w^\mu$ is the nuclear transition energy when the ion is in the electronic state $|\mu\rangle$. $W_{\mu\mu'}$ is the transition probability rate for the transition from $|\mu\rangle$ to $|\mu'\rangle$ ionic spin states.

The amplitude $q_\alpha = a_\alpha + ib_\alpha$ in Eq. (1) is calculated from eigenvectors of *P*:

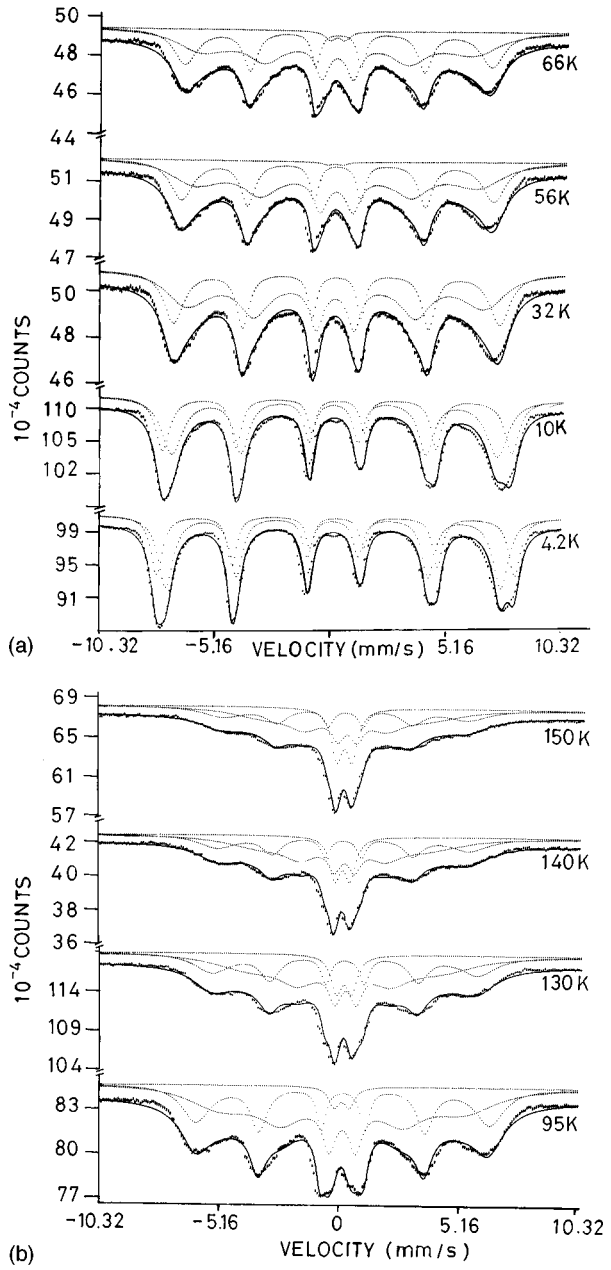

FIG. 1. (a) and (b). Mossbauer spectra of $MgFe_{0.9}Al_{1.1}O_4$. The theoretical spectra which fit best these spectra are shown by solid lines. The component spectra are shown by dotted lines.

$$q_\alpha = \sum_{\mu,\tau=1}^{6} N_\mu T_{\mu\alpha} T_{\alpha\tau}^{-1}, \tag{3}$$

where N_μ is the thermal population of the electronic level μ. T is the 6×6 matrix composed of the eigenvectors $T_{\mu\tau}$ of P, i.e.,

$$T^{-1}PT = D, \tag{4}$$

where D is a diagonal matrix containing the eigenvalues p_α of P.

B. Computation of spectral shapes

The parameters which enter in the computation of relaxation spectra and the procedure of their evaluation are described here.

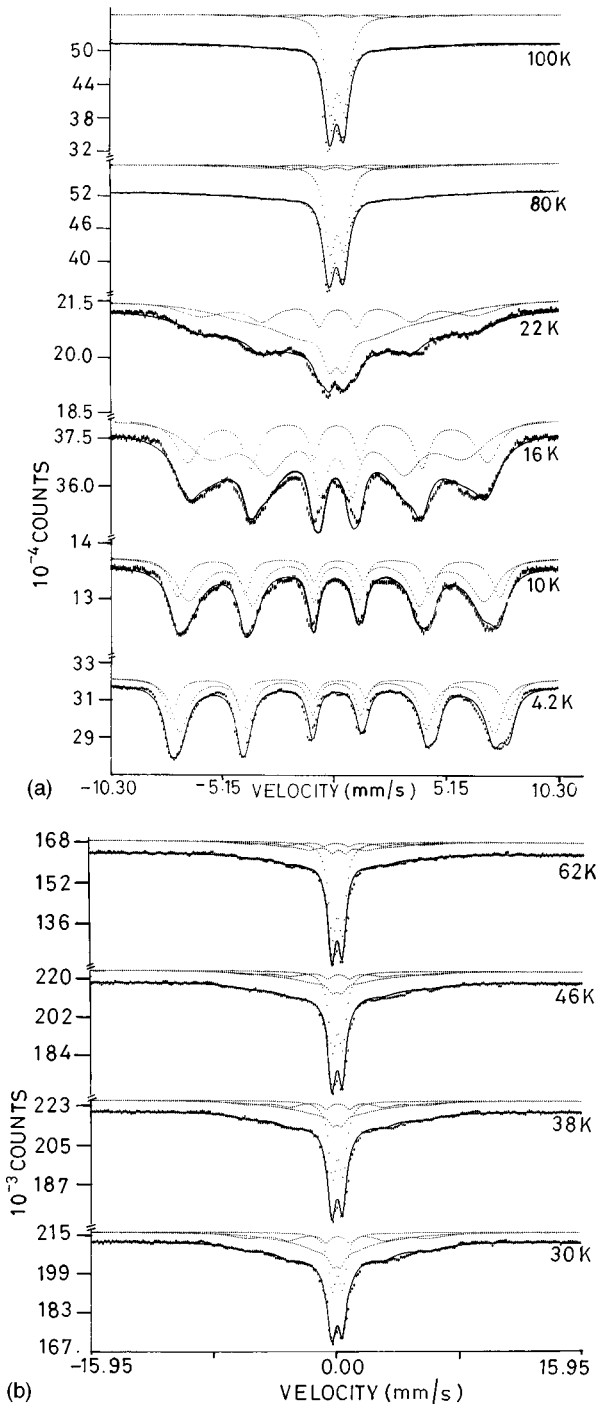

FIG. 2. (a) and (b). Mossbauer spectra of $MgFe_{0.75}Al_{1.25}O_4$. The theoretical spectra which fit best these spectra are shown by solid lines. The component spectra are shown by dotted lines.

(1) The ratio of thermal populations of successive ionic levels, split by Zeeman interaction, is denoted by s. Thus, the thermal populations N_μ of successive levels can be written as $1, s, s^2, s^3$, etc. The thermal average of S_z can be calculated using s:

$$\langle S_z(T)\rangle = \frac{2.5+1.5s+0.5s^2-0.5s^3-1.5s^4-2.5s^5}{1+s+s^2+s^3+s^4+s^5}.$$

(2) The hyperfine magnetic field $H_{\text{int}}(T)$ is proportional to $\langle S_z(T)\rangle$. The hyperfine field at lowest temperature is used to

TABLE II. Results of analyses of Mossbauer spectra of $MgFe_{0.9}Al_{1.1}O_4$ at low temperatures. $H_{int}(A)=474.9$ kG, $H_{int}(B)=515.8$ kG, $\Gamma_{16}:\Gamma_{25}:\Gamma_{34}=0.33:0.32:0.31$ (mm/s), $I_{16}:I_{25}:I_{34}=3.00:2.00:1.00$, $QS(M)_A=0.02$ mm/s, $QS(M)_B=0.03$ mm/s, Relative intensity of A:relative intensity of $B=0.61:0.39$.

Temperature	Component 1 A site		Component 2 B site		Component 3 paramagnetic
(K)	$\langle S_z\rangle$	RT(ns)	$\langle S_z\rangle$	RT(ns)	RI (%)
4.2	2.41	14.75	2.41	4.8	0
10.0	2.23	9.2	2.33	3.3	0
32.0	1.71	7.8	2.14	2.2	0
56.0	1.47	6.3	2.03	1.7	0.6
66.0	1.45	4.6	1.99	1.5	2.2
95.0	1.21	2.7	1.84	1.2	3.75
130.0	1.02	1.4	1.63	1.0	10.0
140.0	0.97	1.1	1.55	0.9	15.0
150.0	0.93	1.1	1.46	0.9	18.8

TABLE III. Results of analyses of Mossbauer spectra of $MgFe_{0.75}Al_{1.25}O_4$ at low temperatures. $H_{int}(A)=466.3$ kG, $H_{int}(B)=524.7$ kG, $\Gamma_{16}:\Gamma_{25}:\Gamma_{34}=0.35:0.33:0.31$ (mm/s), $I_{16}:I_{25}:I_{34}=3.00:2.00:1.00$, $QS(M)_A=0.01$ mm/s, $QS(M)_B=0.02$ mm/s, Relative intensity of A: relative intensity of $B=0.65:0.35$.

Temperature	Component 1 A site		Component 2 B site		Component 3 paramagnetic		
(K)	$\langle S_z\rangle$	RT(ns)	$\langle S_z\rangle$	RT(ns)	QS(P)	CS[a]	RI (%)
4.2	2.36	13.2	2.32	0.8			
10.0	2.13	7.2	2.20	1.0			
16.0	1.52	4.2	2.00	1.3			
22.0	0.74	2.1	1.65	2.2			
30.0	0.58	1.4	1.50	1.6	0.36	0.09	25
38.0	0.64	1.6	1.47	1.5	0.35	0.085	37
46.0	0.69	1.6	1.40	2.0	0.34	0.09	40
62.0	1.01	1.05	1.53	1.2	0.34	0.08	55
80.0	1.14	0.7	1.57	1.0	0.33	0.09	68
100.0	1.20	0.3	1.51	0.4	0.33	0.09	83

[a]Center shift relative to Fe metal in mm/s.

determine the proportionality constant. At low temperature, $|5/2\rangle$ is populated and the lines are narrow. A fit to such a spectrum provides a hyperfine field corresponding to $|5/2\rangle$ and provides the proportionality constant. This field corresponding to $|5/2\rangle$ is also the saturation hyperfine field, $H_{int}(0)$.

(3) At low temperatures, the line broadening due to relaxation is negligible. Consequently, Γ and the relative line intensities of the three pairs of lines in a sextet are obtained by fitting the spectrum at 4.2 K.

(4) The relaxation matrix with elements $W_{\mu\mu'}$, which describe the relaxation frequencies between various ionic levels, depends on the relaxation process. A detailed discussion of various relaxation processes and the associated relaxation frequencies can be found elsewhere.[24,28] At low temperatures, spin-lattice relaxation can be neglected.[28] Only spin-spin relaxation is taken into consideration. The rate of flipping between $|5/2\rangle-|3/2\rangle$, $|3/2\rangle-|1/2\rangle$, and $|1/2\rangle-|-1/2\rangle$ ionic levels due to spin-spin relaxation are 5Ω, 8Ω, and 9Ω, respectively.[24,28] The relaxation time (RT) is related[24,28] to Ω by the relation $RT=[7(1+s)\Omega]^{-1}$.

C. Results

$H_{int}(0)$, Γ, electric quadrupole shifts, relative line intensities of the three pairs of lines in a sextet, and the relative intensities of the two sextets are obtained by fitting the spectra at 4.2 K. These parameters are fixed while fitting the spectra at higher temperatures. Thus, only s, Ω, and center shifts are treated as variable parameters in fitting spectra at higher temperatures. The fit of the experimental data with the computed spectra is shown in Figs. 1 and 2. The results of the analyses are given in Tables II and III. The temperature dependence of the relaxation time of ions at the A site in the composition with $x=0.75$ is shown in Fig. 3. A change occurs in the temperature interval 25–30 K.

1. Cation distribution

It was found in earlier investigations[26] that $CS(A)<CS(B)$, $H_{int}(A)<H_{int}(B)$, and $QS(A)<QS(B)$. The cation distribution in $MgAl_2O_4$ is $(Mg)[Al_2]O_4$.[29] Here, ( ) and [ ] denote ions at the A and B sites, respectively. Thus, Al is known to prefer B sites. $MgFe_2O_4$ is nearly inverse. The cation distribution is found[30] to be $(Mg_{0.04}Fe_{0.96})[Mg_{0.96}Fe_{1.04}]O_4$. Thus, Mg too has a preference for the B site. Based on these known facts, the cation distribution inferred in the oxides under study are

$$(Fe_{0.49}(Mg,Al)_{0.51})[Fe_{0.26}(Mg,Al)_{1.74}]O_4 \quad \text{for } x=0.75,$$

$$(Fe_{0.55}(Mg,Al)_{0.45})[Fe_{0.35}(Mg,Al)_{1.65}]O_4 \quad \text{for } x=0.90.$$

Referring to Fig. 8 of Ref. 22,

$$C_A=0.49, \quad C_B=0.13, \quad \text{when } x=0.75,$$

$$C_A=0.55, \quad C_B=0.175, \quad \text{when } x=0.9.$$

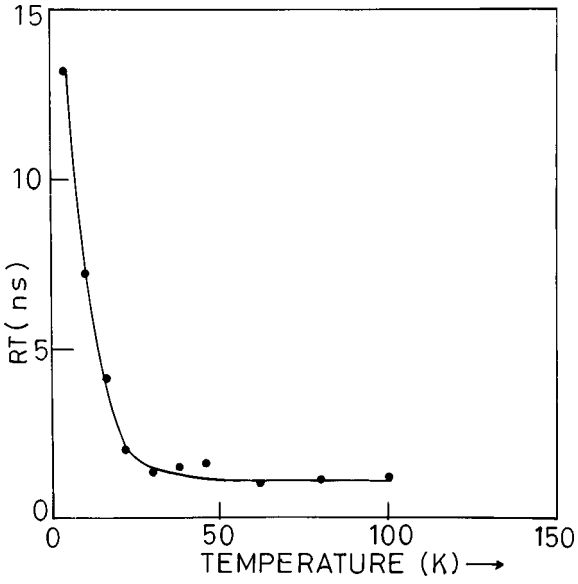

FIG. 3. Temperature dependence of the relaxation time (RT) of Fe ions at A sites in $MgFe_{0.75}Al_{1.25}O_4$.

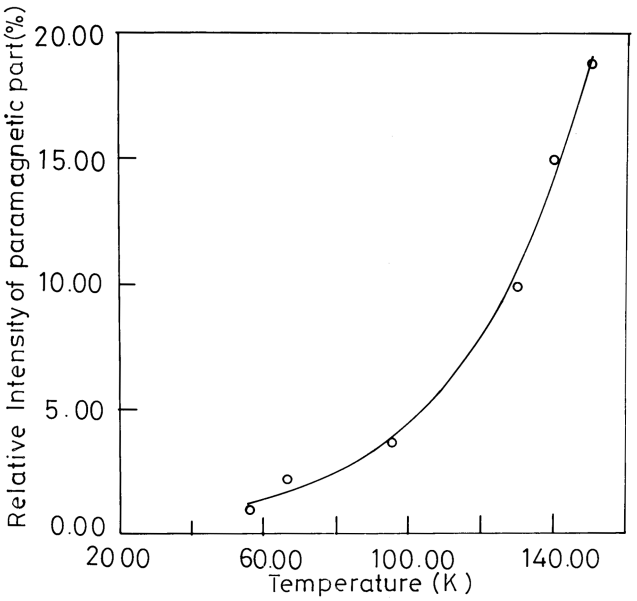

FIG. 4. Temperature dependence of the relative intensity of the paramagnetic component in the spectrum of $MgFe_{0.9}Al_{1.1}O_4$.

The first composition ($x=0.75$) lies very close to the line separating the spin-glass (SG) and localized canted state (LCS) regions.[22] The second composition ($x=0.9$) lies in the LCS region.[22] We, therefore, expect to study the characteristics of the two regions in the present study.

2. Néel temperature

It was found earlier[26] that T_N decreases linearly as the concentration of Fe in $MgFe_xAl_{2-x}O_4$ decreases. The rate is $\approx 35°$ for a change in x by 0.1. We, thus, estimate the transition temperature of the compositions with $x=0.9$ and $x=0.75$ to be 291 and 239 K, respectively. This decrease in T_N with x is not expected to be linear at larger values of x also, but this estimate serves as a guide.

The conversion of the magnetic into the paramagnetic spectrum occurs at T_N in the absence of superparamagnetism. In the oxides under study, however, superparamagnetic effects are present, due to the large concentration of the diamagnetic ions. The conversion of the magnetic into the paramagnetic spectrum, therefore, occurs at temperatures well below T_N (Figs. 4 and 5). Thus, the intensity of the magnetic component is found to become zero at 115 K (Fig. 5) for $x=0.75$. The temperature dependence of $\langle S_Z \rangle$ indicates that the transition temperature is higher than 115 K (Fig. 6). The difference between the temperature at which the magnetic component disappears due to superparamagnetism and T_N is expected to increase with the concentration of the diamagnetic ions. It is, therefore, not possible to determine the Néel temperatures of such oxides using Mossbauer spectroscopy.

3. Ionic magnetization and noncollinear spin structure

Mossbauer spectroscopy enables the determination of $\langle S_Z \rangle$ of Fe ions. The most interesting finding of the present study is the anomalous temperature dependences of the Fe ionic moments at the two sites in these oxides (Figs. 6 and 7). The anomalous behavior is different at the two sites in the lattice. The ions on the sublattice *A*, which are expected to show larger noncollinearity, show more abnormal behavior than the ions on sublattice *B*.

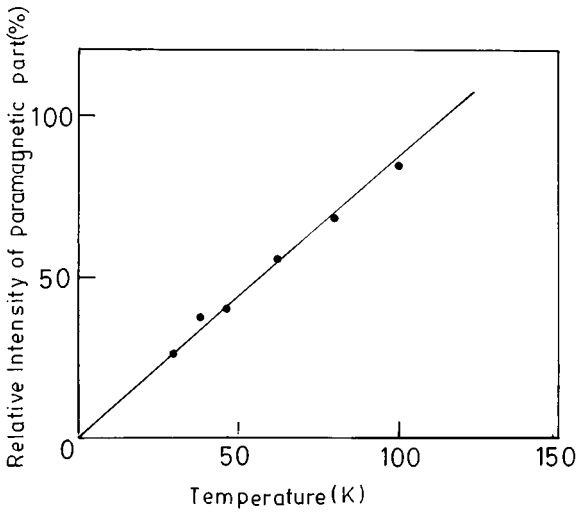

FIG. 5. Temperature dependence of the relative intensity of the paramagnetic component in the spectrum of $MgFe_{0.75}Al_{1.25}O_4$.

The result for $x=0.75$ shows another remarkable characteristic. The magnetization decreases sharply initially as the temperature increases up to 30 K and then rises before finally decreasing again (Fig. 6). It is interesting to note that the FC and ZFC magnetizations for this composition show a peak at 35 and 25 K, in the presence of 50 and 1000 Oe, respectively (Fig. 8). The branching temperature of FC and ZFC magnetizations also lie in this temperature range, and decreases as the field increases. As mentioned above, the temperature dependence of the relaxation time also shows a change at 25–30 K (Fig. 3).

IV. DISCUSSION

The substitution of magnetic ions by diamagnetic cations on a sublattice in a ferrite results in the splitting of the neighboring sublattice into noncollinear sublattices.[1–5] The Yafet-Kittel[1] model of the noncollinear spin structure of fer-

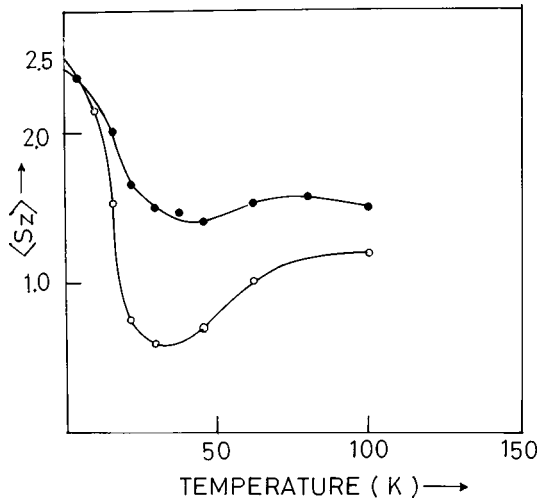

FIG. 6. Temperature dependences of $\langle S_Z \rangle$ of Fe ions at *A* and *B* sites in $MgFe_{0.75}Al_{1.25}O_4$.

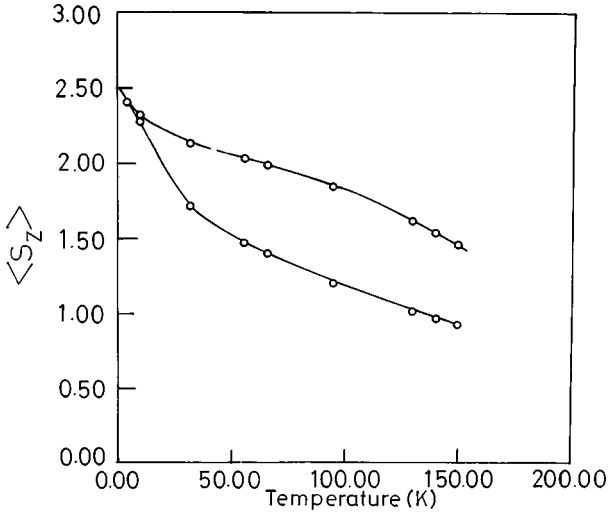

FIG. 7. Temperature dependences of $\langle S_Z \rangle$ of Fe ions at A and B sites in $MgFe_{0.9}Al_{1.1}O_4$.

rites does not take into consideration the variation in the magnetic interactions from site to site on a sublattice. Instead, the two sublattices are assumed to be magnetically homogeneous. Furthermore, noncollinearity with respect to the direction of net magnetization alone is taken into consideration. It can, therefore, be described as a two-dimensional (2D) model. In this model, the A and B sublattices are subdivided into two ($A^{1,2}$) and four subsublattices ($B^{1,2,3,4}$) such that intrasub-sublattice interactions are much weaker than other interactions.[1,2] Consequently, spins on any of the six sublattices mentioned above have no tendency to orient at an angle with respect to each other, but can make angles with respect to ions on other sublattices. The condition for the appearance of noncollinearity on B or A sublattices are[2]

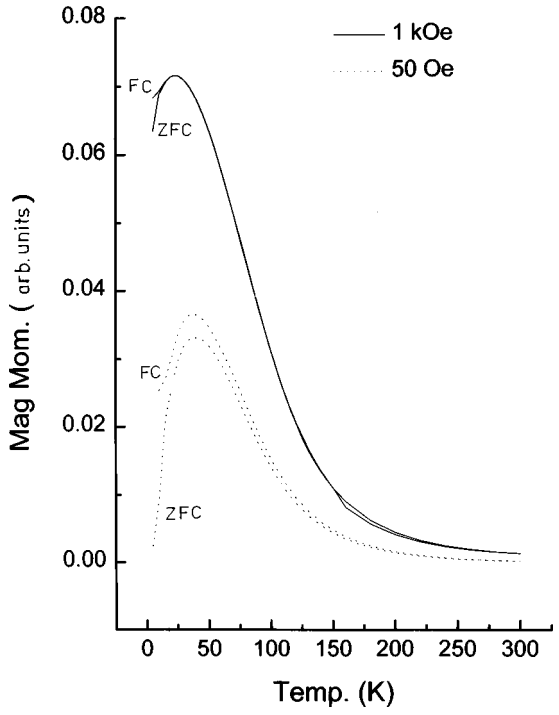

FIG. 8. Temperature dependences of FC and ZFC magnetizations of $MgFe_{0.75}Al_{1.25}O_4$.

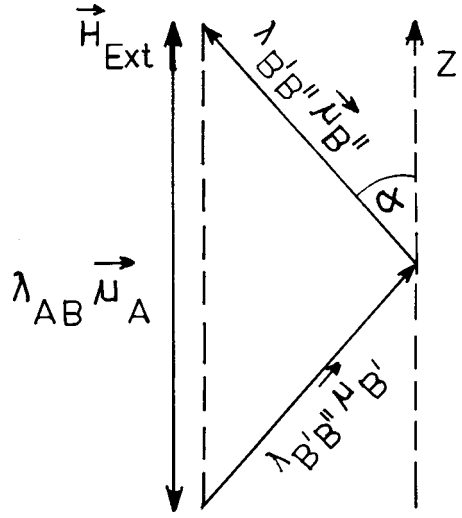

FIG. 9. Schematic representation of noncollinearity on B sublattice, represented by Eq. (5). Similar representation of noncollinearity at A sublattice, represented by Eq. (6), can be drawn.

$$\mathbf{H}_{\mathrm{Ext}} = \lambda_{AB}\boldsymbol{\mu}_A + \lambda_{B'B''}\boldsymbol{\mu}_B \tag{5}$$

or

$$\mathbf{H}_{\mathrm{Ext}} = \lambda_{AB}\boldsymbol{\mu}_B + \lambda_{A'A''}\boldsymbol{\mu}_A , \tag{6}$$

respectively (Fig. 9). Here, $\mathbf{H}_{\mathrm{Ext}}$ is an external magnetic field, and $\lambda_{ij} = (2J_{ij}n_{ij}/g^2\mu_B^2)$. The magnetic energy does not change if B^1 and B^3 as well as B^2 and B^4 are treated as collinear.[2] Thus, the A or B sublattice splits into two sublattices as a result of noncollinearity. It is, thus seen that noncollinearity on a sublattice appears when the intrasublattice interaction becomes greater than the intersublattice interaction (Fig. 9). As a result of the assumption of the magnetic homogeneity of a sublattice, the Yafet-Kittel (YK) model predicts that the noncollinearity appears at one of the sublattices (A or B) only.

The assumption of homogeneity of a sublattice made in the Yafet-Kittel model is, however, not justified, due to the short-range nature of the magnetic interactions in the oxides and the random distribution of the diamagnetic ions on a sublattice. There are two effects of relaxing this assumption. Firstly, the noncollinearity can appear on both sublattices simultaneously. This has been found experimentally earlier.[15,16,26] This is very likely in the oxides under study also, because the diamagnetic substitution is large on both the sublattices. Secondly, there is a variation of noncollinearity from site to site. When the concentration of the diamagnetic ions on a sublattice is large, some ions on the neighboring sublattice have noncollinearity angles greater than 90° also. Such ions are said to have suffered spin reversal.[6] In oxides with such a large concentration of the diamagnetic ions, we can talk of spin orientations resembling spin glass. Finally, it should be pointed out that the Yafet-Kittel model considers noncollinearity with respect to the direction of the net magnetization (z direction) only.[1,2] The spin orientation $\boldsymbol{\phi}$ in the XY plane is not considered, which is also expected to differ from site to site.[19,20]

A. Superparamagnetism

Superparamagnetism is observed when the size of the magnetic particle is small (<200 Å). In this case, the magnetization of the single-domain magnetic particle fluctuates among the directions of the easy magnetization. In presence of uniaxial anisotropy, the magnetization fluctuates among the two directions of easy magnetization with the frequency

$$\Omega_{\mathrm{SPM}}=\Omega_0\exp(-KV/kT). \tag{7}$$

Here, $\Omega_0\approx10^9$ Hz, K is the anisotropy energy per unit volume, and V is the volume of the single-domain magnetic particle. In the oxide under study, the physical size of the particle is not small. However, the presence of a large concentration of the diamagnetic cations in the oxide necessarily results in the formation of small magnetic clusters inside the particles, which show superparamagnetism. When the concentration of the diamagnetic ions is large, these clusters can get fully isolated. In this case, Ω_{SPM} is larger than nuclear precession frequency even at low temperatures. This results in a paramagnetic Mossbauer spectrum, even though ions inside the cluster are magnetically ordered. At higher concentrations of the magnetic ions, these clusters get coupled to each other through one or two exchange bonds. At low temperatures, these clusters order like spins in a spin glass. The system has been described as a cluster spin glass. At higher temperatures, when the thermal energy becomes comparable to the coupling between the clusters, the long-range ordering of clusters break down. Thus, the clusters independently perform superparamagnetic fluctuations at higher temperatures. It was shown in an earlier Mossbauer study that a peak in the temperature dependence of ac susceptibility of such a ferrite appears in the temperature range in which the weak coupling between clusters becomes comparable to the thermal energy.[18] In the present study also, ac susceptibility of $MgFe_xAl_{2-x}O_4$, $x=0.9$, shows[21] a broad peak at 150 K, and Mossbauer spectroscopy shows a rapid increase in the relative intensity of the paramagnetic component above 100 K (Fig. 4). Thus, in the present study also, the peak in the ac susceptibility is found to be due to breaking of long-range ordering of clusters into independent superparamagnetic clusters as the temperature is increased.

The presence of superparamagnetic fluctuations in Mossbauer spectroscopy is shown by the appearance of a paramagnetic doublet whose intensity increases with temperature.[18] For discussing the temperature dependence of the relative intensity of the paramagnetic component, we rewrite Eq. (7) as

$$V=-(kT/K)\ln[\Omega_{\mathrm{SPM}}/\Omega_0]. \tag{8}$$

When Ω_{SPM} becomes greater than 10^9 Hz, the magnetic splitting in Mossbauer spectrum disappears. We denote the corresponding volume at temperature T as $V_C(T)$. Ions in clusters smaller than $V_C(T)$ do not give a magnetic split spectrum at T. $V_C(T)$ is larger at higher T. If T_0 denotes the temperature at which all the clusters contribute to the paramagnetic spectrum only, the largest size of the cluster present can be concluded to be $V_C(T_0)$. If K is independent of T, and clusters of all sizes up to $V_C(T_0)$ are equally probable (*uniform cluster size distribution*), the intensity of the doublet, which results from superparamagnetic fluctuations, is proportional[31] to T. This is found to be the case when $x=0.75$ (Fig. 5). It is also remarkable that the line passes through 0 K, and the conversion to the paramagnetic component is complete at 120 K, implying that the sizes of the clusters are smaller than V_C (120 K). In the case of $x=0.9$, on the other hand, the doublet appears at temperatures higher than 60 K, and the rate of conversion (Fig. 4) increases with temperature in the temperature range up to 150 K. We have not made measurements at higher temperatures, although a sigmoidal variation in the intensity of the doublet with temperature is indicated.

The present study, thus, shows that in the composition which lies on the line separating the SG and LCS region,[22] the sizes of the clusters present is smaller, and the particle size distribution is uniform. On the other hand, in the composition with $x=0.9$, which lies in the LCS region[22] of the composition, the average size of the clusters present is relatively greater, and the size distribution is not uniform, but log normal.

B. The anomalous temperature dependence of magnetization

When the concentration of the magnetic ions in a ferrite is large, the temperature dependence of $\langle S_Z\rangle$ follows the Brioullin curve. As the concentration of the diamagnetic ions increases, anomalous behavior of $\langle S_Z\rangle$ is found.[7–10,15,16] It is found using Mossbauer spectroscopy that $\langle S_Z\rangle$ decreases rapidly initially as the temperature increases until a temperature T_{YK}. At higher temperatures ($T>T_{\mathrm{YK}}$), the decrease in $\langle S_Z\rangle$ with the increase in temperature becomes much slower. T_{YK} is found to coincide with the temperature at which the noncollinear spin structure is found to convert into the ferrimagnetic spin structure.[7–10,15,16] Thus, the temperature dependence of $\langle S_Z\rangle$ determined using Mossbauer spectroscopy can give an indication of the presence of noncollinearity. The results obtained in the present study show that the anomalous behavior of magnetization appears at both sublattices, implying noncollinearity exists at both sublattices, as expected.[15,16] Furthermore, the anomaly is found to be larger at the A site. As the noncollinearity is expected to be larger at the A site, the present study shows that the anomaly is proportional to the noncollinearity. The difference in anomaly at the two sites also shows that a collective fluctuation like superparamagnetism cannot be responsible for the anomaly, because it will affect both sites equally.

In earlier studies,[7–10] the anomaly was found to decrease as the external field increases. The change is large even when the applied field is small.

The results obtained[7–10] for $MgFe_{0.9}Al_{1.1}O_4$ and $Ni_{0.25}Zn_{0.75}FeO_4$, which belong to the LCS class of oxides,[22] show that $\langle S_Z\rangle$ decreases rapidly with an increase in temperature up to 40 K, and then slowly above 40 K. On the other hand, in the case of $MgFe_{0.75}Al_{1.25}O_4$, which lies on the boundary between the spin-glass and LCS class of oxides,[22] $\langle S_Z\rangle$ decreases sharply up to 30 K, and then increases again in the region from 30 to 60 K, before finally decreasing again with the increase in temperature. In the following, we provide an explanation of this anomaly.

In spin glasses, there are several energy minima, representing differing spin configurations, in which the system can settle on lowering the temperature. The system settles in

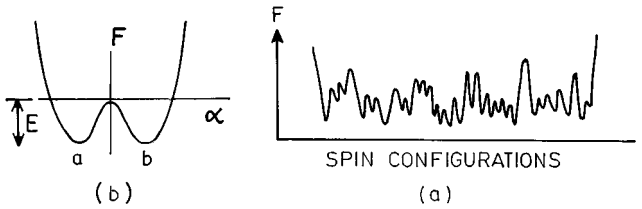

FIG. 10. (a) The free energy of a spin glass in various spin configurations in which the system can settle on lowering the temperature. When the oxide consists of clusters with weak interactions, there are various spin configurations in which the system can settle at low temperatures as explained in the text. The energy of the whole system resembles the energy of a spin glass, consisting a large number of minima and barriers between them. (b) Schematic representation of the change in energy due to interchange of orientations of magnetizations of the two sublattices with respect to the direction of net magnetization, in the Yafet-Kittel model of noncollinear spin structure. The two equivalent spin configurations represented in Fig. 11 are represented as *a* and *b*. The barrier between these configurations decrease as the size of the cluster decreases.

one of these configurations [Fig. 10(a)] at low temperatures. These minima are separated by barriers. We speculate on the configurations corresponding to these energy minima and the energy barriers which separate them in the present system. We assume, for the purpose of the present discussion, that the noncollinearity can be described by the YK model, and appears on the *B* sublattice only. In the formation of the noncollinear spin structure, ions on the sublattice split into two noncollinear sublattices B' and B'', oriented at angles $+\alpha$ and $-\alpha$ to the direction of magnetization of the adjacent sublattice [Fig. 11(a)], respectively. An equivalent configuration is obtained if sublattices B' and B'' are oriented at angles $-\alpha$ and $+\alpha$, respectively [Fig. 11(b)]. The barrier which separates these two equivalent configurations, schematically shown in Fig. 10(b), can be estimated as follows. As can be seen from Fig. 9, the difference in the energies of a *B*-site ion in the two cases, in which the noncollinearity angle is α and zero (Néel's collinear spin arrangement), is given by

$$\Delta E=\lambda_{B'B''}(1-\cos\ \alpha)(\mu_{B'})^2. \tag{9}$$

For the noncollinearity angle of an ion to change from α to $-\alpha$, the Weiss field acting on the ion must change in direction from α to $-\alpha$. This implies that the orientations of all the ions, responsible for the Weiss field, must change sign

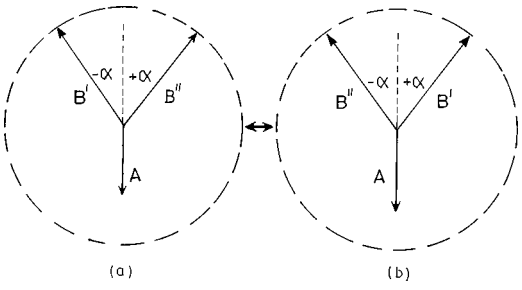

FIG. 11. (a) and (b). Schematic representation of the two equivalent orientations of the two *B* sublattices. When the thermal energy is greater than the barrier between these configurations, there is fast fluctuation between these equivalent configurations.

(from α to $-\alpha$ or vice versa) simultaneously. The barrier to this change is obtained by summing Eq. (9) over all the ions in the cluster:

$$E=\Sigma\tfrac{1}{2}\lambda_{B'B''}(1-\cos\ \alpha)(\mu_{B'})^2. \tag{10}$$

When the thermal energy is greater than this barrier, the flip of the cluster magnetization becomes possible. If the cluster size is small, so that the number of ions required to flip simultaneously is small, the barrier is small. As the thermal energy becomes greater than the height of the barrier, the fluctuations between $-\alpha$ and $+\alpha$ orientations of the ions increase. When the time for which a particular noncollinear ion stays in its orientation is shorter than the nuclear precession period, we observe $\langle S_Z\rangle\cos 2\alpha$, instead of $\langle S_Z\rangle$. The two configurations differ in the orientations of only those ions which are noncollinear, and the effect observed is proportional to the noncollinearity angle α. This is in agreement with the experimental results, as mentioned above. It is, thus, a collective fluctuation like superparamagnetism. In superparamagnetism, the magnetization of all ions flips between up and down directions. In the model proposed here, the moments of all the ions in the cluster flip from $+\alpha$ to $-\alpha$ or $-\alpha$ to $+\alpha$ directions with respect to the lattice magnetization (Fig. 11). Such fluctuations, like superparamagnetism, can also give a peak in ac susceptibility.

As emphasized earlier, the Yafet-Kittel model of noncollinear spin structure is a simplified two-dimensional model. In reality, the energy of a magnetic ion depends on its orientation angles α as well as Φ. Here, α is the angle with respect to the net magnetization, *z* direction, and Φ is the angle in the *XY* plane. The fluctuation of the spins inside the cluster can be between any two equivalent configurations, or even between two configurations which differ in energy and are separated by a barrier, provided the thermal energy is enough to cause the magnetization to jump the barrier. As the temperature increases, the rate of fluctuation increases, which reduces $\langle S_Z\rangle$ to $\langle S_Z\rangle\cos 2\alpha$, where 2α is the angle between the two spin directions between which the fluctuation occurs. Subsequently, the temperature dependence is due to the temperature dependences of $\langle S_Z\rangle$ and α only. Thus, if α decreases rapidly and the change in $\langle S_Z\rangle$ is slower in a temperature range, $\langle S_Z\rangle\cos 2\alpha$ can show an increase, as is observed in the composition with $x=0.75$. The application of an external field reduces the fluctuation rate and, thus, reduces the anomaly in $\langle S_Z\rangle$.

The large number of clusters in a particle, and the possibility of their occurring in different spin orientations, as explained above, makes the system resemble a spin glass. At low temperatures, the system settles in one of the possible configurations. As the temperature increases, fluctuations between different configurations start, as explained above. This gives the anomaly in the temperature dependence of $\langle S_Z\rangle$.

At higher temperatures, superparamagnetic fluctuations start. Ions inside smaller clusters are affected initially. They give a paramagnetic spectrum and stop contributing to $\langle S_Z\rangle\cos 2\alpha$, which is obtained from magnetic spectra. If, as a result, the average of $\cos 2\alpha$ increases, we can see a small increase in $\langle S_Z\rangle\cos 2\alpha$ with an increase in temperature, if the change in $\langle S_Z\rangle$ is small in this temperature range. In the

composition with $x=0.75$, superparamagnetic effects are observable at lower temperatures. It can, therefore, affect $\langle S_Z\rangle\cos 2\alpha$ at lower temperatures. In the composition with $x=0.9$, on the other hand, superparamagnetic effects are confined to a higher temperature range only ($>$100 K). It, therefore, does not affect $\langle S_Z\rangle\cos 2\alpha$ at lower temperatures.

V. CONCLUSIONS

Diamagnetically substituted ferrites in the concentration range in which spin-glass ordering is expected[22] have been investigated using Mossbauer spectroscopy. Anomalous behavior of the ionic magnetization at low temperatures is concluded to be due to fluctuations between equivalent noncollinear spin configurations of the cluster. Such fluctuations are possible when the size of the cluster is small. The nature of spin ordering in the oxide is compared with the spin-glass ordering. At higher temperatures, superparamagnetic effects are present. In $MgFe_{0.75}Al_{1.25}O_4$, the cluster size distribution is found to be uniform. This may be the characteristic feature of an oxide spin glass.

[1] Y. Yafet and C. Kittel, Phys. Rev. **87**, 290 (1952).
[2] F. K. Lotgering, Philips Res. Rep. **11**, 190 (1956).
[3] J. Piekoszewski, L. Dabrowski, J. Suwalski, and S. Makolagwa, Phys. Status Solidi A **39**, 643 (1977).
[4] A. Rosencwaig, Can. J. Phys. **48**, 2857 (1970); **48**, 2868 (1970).
[5] J. M. Daniels and A. Rosencwaig, Can. J. Phys. **48**, 381 (1970).
[6] A. H. Morrish and P. E. Clark, Phys. Rev. B **11**, 278 (1975).
[7] S. C. Bhargava, S. Morup, and J. E. Knudsen, J. Phys. (Paris), Colloq. **37**, C6-93 (1976).
[8] S. C. Bhargava, J. E. Knudsen, and S. Morup, J. Phys. C **12**, 2879 (1979).
[9] S. C. Bhargava and N. Zeman, Phys. Rev. B **21**, 1726 (1980).
[10] S. C. Bhargava and N. Zeman, Phys. Rev. B **21**, 1717 (1980).
[11] R. J. Borg and C. E. Violet, J. Phys. Chem. Solids **48**, 1239 (1987).
[12] F. Varret, A. Hamzic, and I. A. Campbell, Phys. Rev. B **26**, 5285 (1982).
[13] I. A. Campbell, S. Senoussi, F. Varret, J. Teillet, and A. Hamzic, Phys. Rev. Lett. **50**, 1615 (1983).
[14] J. Lauer and W. Keune, Phys. Rev. Lett. **48**, 1850 (1982).
[15] J. L. Dormann, M. El Harfaoui, M. Nogues, and J. Jove, J. Phys. C **20**, L161 (1987).
[16] R. A. Brand, H. Georges-Gibert, J. Hubsch, and J. A. Heller, J. Phys. F **15**, 1987 (1985).
[17] V. Manns, R. A. Brand, W. Keune, and R. Marx, Solid State Commun. **48**, 811 (1983).
[18] S. C. Bhargava, F. M. Mulder, R. C. Thiel, and S. K. Kulshreshtha, Hyperfine Interact. **54**, 459 (1980).
[19] M. R. Singh and S. C. Bhargava, Solid State Commun. **90**, 183 (1994).
[20] M. R. Singh and S. C. Bhargava, J. Phys.: Condens. Matter **7**, 8183 (1995).
[21] M. R. Singh and S. C. Bhargava, Solid State Physics (India) **38C**, 139 (1995).
[22] J. L. Dormann and M. Nogues, J. Phys.: Condens. Matter **2**, 1223 (1990).
[23] S. C. Bhargava and P. K. Iyengar, Phys. Status Solidi B **46**, 117 (1971); **53**, 359 (1972).
[24] S. C. Bhargava, J. Phys. C **19**, 745 (1986).
[25] S. C. Bhargava, J. Phys. (Paris), Colloq. **49**, C8-1051 (1988).
[26] M. D. Sundararajana, A. Narayanasamy, T. Nagarajan, L. Haggstrom, C. S. Swamy, and K. V. Ramanujachary, J. Phys. C **17**, 2953 (1984).
[27] M. J. Clauser, Phys. Rev. B **11**, 3748 (1971).
[28] S. C. Bhargava, J. E. Knudsen, and S. Morup, J. Phys. C **12**, 2879 (1979).
[29] T. Birchall and A. F. Reid, J. Solid State Chem. **6**, 411 (1973).
[30] E. De Grave, A. Govaert, D. Chambaere, and G. Robbrecht, Physica B & C **96**, 103 (1979).
[31] P. Roggwiller and W. Kundig, Solid State Commun. **12**, 901 (1973).